HHS Public Access

Author manuscript

Cancer Immunol Res. Author manuscript; available in PMC 2016 July 01.

Published in final edited form as:

Cancer Immunol Res. 2015 July ; 3(7): 815–826. doi:10.1158/2326-6066.CIR-15-0054.

Generation of Potent T-cell Immunotherapy for Cancer using DAP12-based, Multichain, Chimeric Immunoreceptors

Enxiu Wang, PhD[1], **Liang-Chuan Wang, PhD**[2], **Ching-Yi Tsai, PhD**[1], **Vijay Bhoj, MD, PhD**[1], **Zack Gershenson**[4], **Edmund Moon, MD**[2], **Kheng Newick, PhD**[2], **Jing Sun, MD**[2], **Albert Lo**[3], **Timothy Baradet**[1], **Michael D. Feldman, MD, PhD**[1], **David Barrett, MD, PhD**[4], **Ellen Puré, PhD, AB**[3], **Steven Albelda, MD**[2], and **Michael C. Milone, MD, PhD**[1]

[1]Department of Pathology and Laboratory Medicine, Perelman School of Medicine at the University of Pennsylvania, Philadelphia, PA 19104

[2]Department of Medicine, Perelman School of Medicine at the University of Pennsylvania, Philadelphia, PA 19104

[3]Department of Animal Biology, University of Pennsylvania School of Veterinary Medicine, Philadelphia, PA 19104

[4]Department of Pediatrics, University of Pennsylvania School of Medicine

Abstract

Chimeric antigen receptors (CAR) bearing an antigen-binding domain linked in *cis* to the cytoplasmic domains of CD3ζ and costimulatory receptors have provided a potent method for engineering T-cell cytotoxicity towards B-cell leukemia and lymphoma. However, resistance to immunotherapy due to loss of T-cell effector function remains a significant barrier, especially in solid malignancies. We describe an alternative chimeric immunoreceptor design in which we have fused a single-chain variable fragment for antigen recognition to the transmembrane and cytoplasmic domains of KIR2DS2, a stimulatory killer immunoglobulin-like receptor (KIR). We show that this simple, KIR-based CAR (KIR-CAR) triggers robust antigen-specific proliferation and effector function *in vitro* when introduced into human T cells with DAP12, an immunotyrosine-based activation motifs (ITAM)-containing adaptor. T cells modified to express a KIR-CAR and DAP12 exhibit superior antitumor activity compared to standard first and second generation CD3ζ-based CARs in a xenograft model of mesothelioma highly resistant to immunotherapy. The enhanced antitumor activity is associated with improved retention of chimeric immunoreceptor expression and improved effector function of isolated tumor-infiltrating

Address correspondences to: Michael C. Milone, MD, PhD, Assistant Professor of Pathology and Laboratory Medicine, Hospital of the University of Pennsylvania, 7.103 Founders Pavilion, 3400 Spruce Street, Philadelphia, PA 19104, milone@mail.med.upenn.edu.

Author contributions: EW and LW conceived, designed and performed experiments and analyzed data. VB, EM, CT, TB, AL, KN, JS, ZG, DB and MDF performed experiments. EP supervised experiments. SA conceived and designed experiments, analyzed data and edited the manuscript. MCM conceived and designed experiments, analyzed data, and wrote the manuscript.

Competing interests: EW and MCM have filed a patent application (PCT/US2014/029983) on technology presented in this manuscript.

Data and materials availability: Plasmids and lentiviral vectors encoding the KIR-based CARs as well as some of cell lines described in this manuscript are available to interested investigators, but their availability will depend upon the execution of a material transfer agreement with the University of Pennsylvania.

lymphocytes. These results support the exploration of KIR-CARs for adoptive T-cell immunotherapy, particularly in immunotherapy-resistant solid tumors.

Keywords

immunotherapy; cancer; T cell; CAR; immunoreceptor

Introduction

"First generation" chimeric antigen receptors (CAR) incorporate a cytoplasmic domain containing one or more immunotyrosine-based activation motifs (ITAM) into a single chimeric receptor that uses a single-chain variable fragment (scFv) for antigen recognition (1). Cytoplasmic domains from receptors such as CD28, ICOS, 4-1BB and OX-40 incorporated into these receptors enhance the proliferation, survival and function of T cells (2–5). T cells expressing "second generation" (one co-stimulatory domain) and "third generation" (two co-stimulatory domains) CARs exhibit enhanced function in preclinical animal models of cancer, and T cells bearing several co-stimulation-enhanced CARs are in human clinical trials for cancer (reviewed in (6)).

Although CARs based upon a single chimeric molecule design trigger antigen-specific T-cell responses, natural immunoreceptors are typically structured as multi-chain complexes composed of separate ligand-binding and ITAM-containing signaling chains such as the T-cell receptor (TCR)-CD3 complex (7). The potential benefits of a multi-chain immunoreceptor complex are manifold, including greater diversity of signals available through the multiple interactions between ligand-binding and signaling molecules, and sustained ITAM signaling that is separable from the internalization of the ligand-binding chain (8). The consequence of combining several receptor components normally found in heterologous molecules into a single CAR has not been fully elucidated; however, antigen-independent signaling and induction of anergy have been observed with existing CARs (5, 9, 10).

We hypothesized that a CAR constructed using a natural multi-chain immunoreceptor design would have greater activity in T cells due to the naturally-selected interactions between subunits within the receptor complex and other receptors within immune cells. We chose the killer immunoglobulin-like receptor (KIR) and DAP12 multi-chain immunoreceptor complex as the foundation for a CAR (11). KIR expression is observed in both $CD4^+$ and $CD8^+$ T cells, in addition to NK cells, in which these receptors contribute to natural cytotoxicity (12–14). Activating KIRs, such as KIR2DS2, possess a short cytoplasmic domain with no known signaling activity. However, KIRs form a non-covalent complex with DAP12, an ITAM-containing molecule capable of binding Syk and Zap70 kinases, through transmembrane-mediated interactions (15). In addition to stimulating cytotoxicity upon ligand binding, KIRs have been reported to costimulate T cells in the absence of DAP12 expression suggesting that these molecules may provide both primary triggering activity and costimulation in T cells (16).

We show that a KIR-based CAR (KIR-CAR) targeting tumor-associated antigens can potently activate T cells. Adoptively transferred T cells engineered to express these KIR-CARs and DAP12 can also induce regression of tumor xenografts including a mesothelioma xenograft resistant to treatment with T cells bearing CD3ζ-based CARs with 4-1BB or CD28 costimulatory domains.

Materials and Methods

Anti-mesothelin and CD19-specific KIR-CARs

Mesothelin and CD19-specific CD3ζ-based CARs, SS1ζ, SS1-28ζ, SS1-BBζ, CD19ζ and CD19-BBζ, used for all studies were those previously described (4, 5). The lentiviral vector expressing Dap12-T2A-SS1-KIRS2 was constructed using standard molecular biology techniques. First, Dap12 cDNA cloned from human peripheral blood mononuclear cells (PBMC) was used as a template for PCR amplification of the 351-bp complete coding sequence for Dap12 using the following primers: 5_-TCTAGAATGGGGGGACTTGAAC-_3 (XbaI/ is underlined), 5_-GTCGACTTTGTAATACGGCCTC_-3 (SalI/ is underlined). The resulting PCR product was cloned in-frame 3′ to a dsRed-*Thoseasigna* virus 2A (T2A) fusion sequence downstream of the EF-1α promoter in the previously described 3rd generation self-inactivating lentiviral vector (5) to generate pELNS Dap12-T2A-dsRed. The mesothelin scFv (SS1), previously described (4) was used as a template for PCR amplification of the 801-bp SS1 fragment using the following primers: 5_-CCTAGGATGGCCTTACCAGTG-_3 (AvrII/ is underlined), 5_-GCTAGCTTTGATTTCCAACTTTGTCC-_3 (NheI/ is underlined). The resulting PCR product containing the SS1 scFv coding sequence was ligated to a 270-bp PCR product from KIR2DS2 generated by PCR from cDNA using the following primers: 5_-GCTAGCGGTGGCGGAGGTTCTGGAGGTGGGGGTTCCTCACCCACTGAACCAAGC_-3 (NheI/ is underlined), and 5′_- GTCGACTTATGCGTATGACACC_-3 (SalI/ is underlined). The resulting chimeric SS1 scFv-KIR2DS2 fragment (termed SS1-KIRS2) was subsequently cloned in-frame 5′ to the Dap12-T2A sequence in pELNS Dap12-T2A-dsRed to generate pELNS Dap12-T2A-SS1-KIRS2. CD19-KIRS2/Dap12 and FAP-KIRS2/Dap12 vector inserts were made by exchanging the SS1 scFv with a CD19-specific scFv sequence derived from FMC63 previously described (5) and FAP-specific scFv previously described (17) at BamHI and NheI sites, respectively. High-titer replication-defective lentiviral vectors were produced and concentrated as previously described (5).

Isolation, Transduction, and Expansion of Primary Human T Lymphocytes

Primary human T (CD4 and CD8) cells were isolated from healthy volunteer donors following leukapheresis by negative selection using RosetteSep kits (Stem Cell Technologies). All specimens were collected under a University Institutional Review Board-approved protocol, and written informed consent was obtained from each donor. T cells were cultured in RPMI 1640 supplemented with 10% FCS, 100-U/ml penicillin, 100-g/ml streptomycin sulfate, 10-mM Hepes, and stimulated with magnetic beads coated with anti-CD3/anti-CD28 at a 1:3 cell to bead ratio. Approximately 24 h after activation, T cells were transduced with lentiviral vectors at an MOI of 3 to 6. Cells were counted and fed every 2 days until they were either used for functional assays or cryopreserved after rest down.

Flow Cytometric Analysis

Target cells, K562 (Kwt), K562.meso (Kmeso), EM parental (EMp) and EM-meso cells were stained for surface expression of mesothelin using the CAK1 antibody (clone K1, Covance) followed by PE-labeled secondary goat-anti-mouse antibody. Expression of the various SS1 scFv fusion proteins on T cells was detected using either biotinylated goat anti-mouse $F(ab)_2$ (Jackson ImmunoResearch) followed by staining with streptavidin-PE (BD Biosciences), or with a mesothelin-V5-hisx12 fusion protein (kindly provided by Jennifer Brogdon, Novartis Institute of Biomedical Research) followed by staining with a V5 eptitope-specific, FITC-conjugated antibody (Thermo Scientific). Samples were analyzed on either LSRII or FACSCalibur flow cytometers (BD Biosciences) and analyzed with FlowJo software (TreeStar).

Chromium Release Assay

Target cells were loaded with ^{51}Cr and combined with differing amounts of transduced T cells in U-bottom plates. After a 4-h incubation at 37°C, the release of free ^{51}Cr was measured using a COBRA II automated gamma-counter (Packard Instrument Company). The percent-specific lysis was calculated using the formula: % specific lysis = 100 x (experimental cpm release – spontaneous cpm release)/(total cpm release – spontaneous cpm release). All data are presented as a mean±standard deviation of triplicate wells.

Immunohistochemistry

Two color immunohistochemical staining for human CD8 alpha (Clone C8/144B; Dako M7103; 1:100 dilution) and mesothelin (Clone 5B2, Thermo Scientific MS-1320; 1:30 dilution) was performed sequentially on a Leica Bond III using the Bond Polymer Refine Detection System and the Bond Polymer Refine Red Detection System. Heat-induced epitope retrieval was done for 20 minutes with ER2 solution (Leica Microsystems AR9640). Following dual color immunohistochemistry, multispectral imaging was performed on the stained sections using a Vectra multispectral imaging system (Perkin Elmer, Waltham MA) and the resulting multispectral images were analyzed using InForm Imaging software (Perkin Elmer, Waltham MA). Ten random 20x fields were selected for analysis of each tumor. The images were segmented into tumor and stromal regions using mesothelin staining and morphologic features of the tumor cells from the hematoxylin counterstain using Informs “train by example” segmentation algorithm. $CD8^+$ T-cell counting was then performed by counting $CD8^+$ T cells within tumor and stromal regions.

Bioluminescent imaging of Leukemia

Nalm6 leukemic cells transduced with Click Beetle Luciferase emitting in the green spectrum (CBG, λ_{peak} 550 nm, Chrom-Luc Green, Promega) were injected into adult NSG mice on day 0 as previously described (18). T cells with or without CARs were injected on day 5, and the tumor burden was assessed by imaging anesthetized mice using a Xenogen Spectrum system and Living Image v4.2 software following intraperitoneal injection of 150 mg/kg D-luciferin (Caliper Life Sciences, Hopkinton, MA). Each animal was imaged alone (for photon quantification) or in groups of up to five mice (for display purposes) in the anterior–posterior prone position at the same relative time point after luciferin injection (6

min). Data were collected until the midrange of the linear scale was reached (600–60,000 counts) or maximal exposure settings reached (f stop 1, large binning, and 120 sec), and then converted to photons/sec/cm2/steradian to normalize each image for exposure time, f-stop, binning, and animal size.

Tumor-infiltrating lymphocytes (TIL) isolation and enrichment

Tumors were harvested at various time points and processed as previously described (19). In brief, tumors were harvested, micro-dissected into small fragments, and then digested for 1 hour at 37°C with a cocktail of collagenase type I (1U/10mL, Worthington), II (1U/10mL, Worthington) and IV (1U/10mL, Worthington), DNase I (0.5U/10mL, Worthington), and elastase (0.5U/10mL, Worthington), in L15-medium (10mL per tumor; Leibovitz). Digested tumors were then filtered through 70-μm nylon mesh cell strainers, and red blood cells were lysed prior to analysis by flow cytometry (BD Pharm Lyse; BD Biosciences). For functional analysis and western blotting experiments, further purification of the TILs was performed. Dead cells were first removed by labeling with anti-phosphotidylserine microbeads (#130-090-101; Miltenyi Biotec) to avoid non-specific binding of antibody to dead cells during the TIL enrichment process. The live single-cell suspension was then blocked with anti-mouse CD16/CD32 antibody for 15 minutes, followed by staining with phycoerythrin-conjugated anti-human CD45 (3 μg/ml as the final concentration; BD Biosciences) for an additional 20 minutes. Human T cells were then targeted with tetrameric antibody complexes (EasySep PE selection kit, #18551, STEMCELL Technologies) recognizing PE and dextran-coated microbeads. Labeled cells were positively selected using an EasySep magnet. The purity of isolated TILs were then confirmed by flow cytometry, and >90% purity were achieved throughout the entire study. Cryopreserved T cells expressing CD3ζ-based and KIR-based CARs were processed using the same TIL isolation procedure described with no effect on CAR expression as assessed by either flow cytometry for surface expression (data not shown) or immunoblotting for CD3ζ (Supplemental Fig 7).

Functional assessment of isolated TILs

TILs were co-cultured with firefly luciferase-expressing tumor cells at different effector TIL to target (E:T) ratios for a specified period of time. At the end of the co-culture incubation period, supernatant was saved for IFNγ concentration measurement by ELISA (Biolegend #430106), wells were washed, and remaining adherent tumor cells were lysed with a 1X cell lysis buffer for 30 minutes. Luciferase activity in the lysates was analyzed using the Luciferase Assay System on a GloMax Multi Detection System (Promega.) Results are reported as percent-killing based on luciferase activity in wells with tumor, but no T cells. (% killing = 100-((RLU from well with effector and target cell coculture)/(RLU from well with target cells)×100)). Effector-to-target ratios represent total T cells per target cell.

TIL immunoblotting

For immunoblot analysis, 1.5 million T cells or isolated TILs were lysed with RIPA buffer supplemented with a protease inhibitor cocktail (Roche). Whole cell lysates (20μg per sample) were separated by SDS-PAGE, transferred to nitrocellulose membranes, and probed with antibodies specific for target proteins as indicated followed by goat-anti-rabbit or goat-anti-mouse secondary antibodies conjugated to alkaline phosphatase. Binding was detected

by chemiluminescence using Westerj Lighting Plus-Enhanced Chemiluminescence Substrate, (NEL104001EA; Perkin Elmer).

Statistical Analysis

Statistical analyses were performed using STATA version 12 (STATAcorp, College Station, TX). Unless indicated, a one-way analysis of variance was performed in experiments involving multiple comparisons of groups with a threshold p-value of <0.05 prior to performance of post hoc analysis by the Scheffe F-test.

Results

Construction of a KIR-CAR with DAP12-dependent cytotoxic activity

A KIR-CAR was constructed by splicing a mesothelin-specific SS1 scFv antibody onto the transmembrane and short cytoplasmic domain of KIR2DS2 (SS1-KIRS2) as illustrated schematically in Figure 1A. DAP12 is constitutively expressed in NK cells, but it is only expressed in a subset of human T cells (12). We therefore generated a bicistronic, lentiviral vector encoding SS1-KIRS2 and DAP12 separated by the *Thoseasigna* virus 2A (T2A) sequence in order to achieve co-expression of both molecules (Fig. 1B). Transduction of primary human T cells with this bicistronic lentivirus following anti-CD3 and anti-CD28 activation yields surface expression of SS1-KIRS2 that is comparable to the CD3ζ-based SS1ζ CAR (Fig 1C). SS1-KIRS2/DAP12-transduced T cells expand following anti-CD3 and anti-CD28 agonist antibody stimulation with kinetics comparable to mock-transduced T cells (data not shown). SS1-KIRS2/DAP12 triggers potent *in vitro* T-cell cytotoxic activity towards K562 cells that express human mesothelin (Kmeso) with similar magnitude to SS1ζ. None of the engineered T cells demonstrate lytic activity towards wild-type K562 (Kwt) supporting the specific activation of the SS1-KIRS2/Dap12 receptor by the cognate mesothelin target antigen (Fig 1D). Since T cells express KIR2DS2 in the absence of detectable DAP12 expression, we evaluated SS1-KIRS2 receptor expression and function with and without co-delivery of DAP12. As expected, SS1-KIRS2 is expressed on the surface of T cells without the addition of DAP12; however, T cells expressing SS1-KIRS2 without co-transduction of DAP12 fail to lyse mesothelin-expressing target cells demonstrating a requirement for co-delivery of DAP12 for SS1-KIRS2-triggered T-cell cytotoxic activity (Supplemental Fig 1). These data do not preclude the possibility that a chimeric KIR provides signals independently of its association with DAP12 as previously reported for the natural KIR2DS2 receptor in T-cell clones (16).

The non-covalent association of KIR2DS2 and DAP12 depends upon the electrostatic interactions between an aspartic acid residue in the KIR transmembrane (TM) domain and a lysine residue in the DAP12 TM domain. Although the position of the ionizable residues within the hydrophobic TM domains of multi-chain immunoreceptors appear to direct the specificity of these receptor interactions, we explored the possibility that SS1-KIRS2 expression in the absence of DAP12 co-delivery might be due to interactions with components of the endogenous CD3 complex expressed by T cells, which shares a similar mechanism of TM interaction for complex assembly and surface expression (20). The introduction of an ectopic Vβ chain into T cells has been shown to reduce the surface

expression of endogenous TCR Vβ due to competition during complex assembly (21, 22). We observed a similar frequency and intensity of TCR Vβ 13.1+ in SS1-KIRS2-transduced polyclonal T cells compared with mock-transduced, control T cells supporting the absence of a significant interaction between SS1-KIRS2 and members of the endogenous CD3 complex (Supplemental Fig 2).

A KIR-CAR/Dap12 induces cytokine production and proliferation without the need for further co-stimulation

Cytokine secretion and T-cell proliferation are important characteristics that are generally dependent upon co-stimulation and correlate with robust antitumor activity *in vivo*. We compared the antigen-triggered secretion of interferon-γ (IFNγ) and interleukin-2 (IL2) by SS1-KIRS2/DAP12-modified T cells with T cells bearing a CD3ζ-based CAR without a costimulatory domain (SS1-ζ) or with CD28 or 4-1BB co-stimulatory domains (SS1-28ζ and SS1-BBζ, respectively) (4). As expected, SS1-ζ stimulates the lowest secretion of IFNγ and IL2 (Fig 2A, B). Interferon-γ production is increased and comparable in T cells expressing SS1-KIRS2/DAP12 or SS1-BBζ whereas T cells expressing the SS1-28ζ CAR show significantly greater IL2 and IFNγ production (Fig. 2A). Analysis of a larger panel of cytokines and chemokines demonstrates that SS1-KIRS2/DAP12 stimulates a pattern of expression that is qualitatively similar across CD3ζ-based CARs with a magnitude of antigen-induced cytokine and chemokine secretion that is comparable to SS1-ζ and SS1-BBζ CARs (Fig 2B).

The SS1-KIRS2/DAP12 receptor is also a potent stimulator of T-cell proliferation in response to cognate antigen (Fig 2C). Stimulation of SS1-ζ CART cells with mesothelin-expressing cells resulted in minimal T-cell proliferation as previously demonstrated with 1st-generation CD3ζ-based CARs (5, 23–26). Proliferation could be enhanced in the presence of soluble anti-CD28 agonist antibody. In contrast, SS1-KIRS2/DAP12 induced proliferation in response to mesothelin antigen that was comparable to SS1ζ with addition of anti-CD28 agonist antibody with no evidence of increased proliferation with the addition of anti-CD28 agonist.

KIR-CARs/Dap12 show potent antitumor activity in vivo

CD28 and 4-1BB have been incorporated into CARs to enhance CAR T-cell activity *in vivo* (4); however, costimulation is not always able to overcome the immunosuppressive tumor microenvironment (TME). We recently reported that SS1-BBζ CAR T cells injected into immunodeficient NOD-SCID-$\gamma_c^{-/-}$ (NSG) mice bearing a xenograft of EM-meso cells (a cell line derived from the pleural effusion of a patient with malignant mesothelioma) expand *in vivo*, but become hypofunctional within the TME associated with failure to clear tumors (19). We evaluated the activity of SS1-KIRS2/DAP12-modified T cells in this T-cell immunotherapy-resistant model of mesothelioma. SS1-KIRS2/DAP12- and CD3ζ-based CARs with or without costimulation lyse EM-meso target cells *in vitro* with comparable efficacy. Mock-transduced and DAP12-dsRed-transduced T cells show minimal lytic activity towards EM-meso cells (Supplemental Fig 3). A single intravenous injection of 5 million mock, SS1ζ–, or SS1BBζ-transduced T cells had no observable antitumor effect on established EM-meso xenografts (Fig 3A). Tumor growth was slightly, but statistically

significantly delayed by T cells expressing SS1-28ζ; however, only SS1-KIRS2/DAP12-modified T cells induced regression of tumors with significant suppression of EM-meso tumor growth at 52 days ($p < 0.001$, ANOVA with post-hoc Scheffe F-test). A second experiment comparing T cells expressing SS1-KIRS2/DAP12 to DAP12 alone or SS1-28ζ engineered T cells showed similar enhanced antitumor activity of SS1-KIRS2/DAP12 T cells (Supplemental Fig 4).

To determine if the potent antitumor activity of T cells bearing a KIR- CAR/Dap12 is unique to the mesothelin-specificity, we generated additional KIR-based CARs targeting CD19 and fibroblast activation protein (FAP). T cells expressing a CD19-specific KIRS2-based CAR with DAP12 (CD19-KIRS2/DAP12) showed *in vitro* cytotoxic activity that was comparable to previously described CD3ζ–based CARs (Supplementary Fig 5) (5). In a NALM-6 B-cell leukemia xenograft model, T cells expressing CD19-KIRS2/DAP12 achieve superior control of leukemia when compared to a first generation CD19-specific CAR bearing only a CD3ζ cytoplasmic domain (19ζ). CD19-KIRS2/DAP12-modified T cells exhibited control of leukemia that was comparable to a second generation CD19-specific CAR with the 4-1BB costimulatory domain (CD19-BBζ) that has been shown to have potent anti-leukemic activity in humans (Fig 3B) (27, 28). The similar *in vivo* activity of CD19-KIRS2/DAP12 CAR T cells and CD19-BBζ CAR T cells in this model confirms the enhanced activity of KIR-CARs/Dap12 without the incorporation of additional costimulatory signals.

Unlike mesothelin and CD19, FAP, while expressed on the surface of some tumors such as osteosarcoma (29), is expressed within a range of tumors by stromal cells in the TME including tumor-associated fibroblasts (TAF) and tumor-associated macrophages (TAM) (30, 31). These stromal cells support tumor growth and limit immunologic reactions against the tumor (32). Targeting FAPs has therefore been proposed as an adjunct to tumor-targeted therapy to deplete these FAP^+ stromal cells (17, 33–36). We generated a murine FAP-specific KIR-based CAR (FAP-KIRS2) using the scFv from the 73.3 hybridoma that was previously described by our group in a CD3ζ-based FAP-specific CAR bearing the 4-1BB costimulatory domain (FAP-CAR) (17). T cells expressing FAP-KIRS2 and DAP12 (FAP-KIRS2/DAP12) show antigen-specific cytotoxicity *in vitro* that is comparable to T cells expressing CD3ζ-based CARs (data not shown). As we have seen in a mouse model of human lung cancer (38), when we treated established human EM-meso tumors growing in NSG mice with the CD3ζ-based FAP-CAR construct, we observed a significant, but modest slowing of tumor growth, and no toxicity (Fig 3C). However, when the same tumors were treated with the FAP-KIRS2/DAP12-modified T cells, a much more marked antitumor effect was observed, with tumor growth completely halted (Fig 3D). Interestingly, after using these effective FAP-KIRS2/DAP12-modified T cells, we now observed anemia (Fig 3E) along with hypocellularity of the bone marrow and weight loss (Supplemental Fig 6). This is similar to toxicity reported in a genetic model of complete FAP ablation (37). These effects can be explained by a more complete depletion of the intra-tumoral $CD45^-$/$CD90^+$/FAP^+ and $CD45^+$/FAP^+ cells within the treated tumors (Fig 3F) than observed in our previously studies with CD3ζ-based FAP-specific CARs (17).

Overall, these data show that the KIR-based CAR platform is a potent CAR design for generating tumor-directed T-cell immunotherapy with significantly enhanced antitumor activity over 2nd generation CD3ζ-based CARs in some settings. Understanding the mechanism for this enhanced activity is therefore critical to understanding this new CAR design and perhaps improving existing CD3ζ-based CAR designs.

The enhanced in vivo activity of T cells with a KIR-CAR/Dap12 is associated with better maintenance of CAR expression in TILs

To explore the mechanism of the enhanced antitumor activity of the mesothelin-specific SS1-KIRS2/DAP12 T cells compared with CD3ζ-based mesothelin-specific CARs in the EM-meso xenograft model, an analysis of T-cell engraftment and TILs was performed. Few $hCD45^+$ TILs were detected in mock or SS1ζ-treated mice from the experiment shown in Fig 3A. In contrast, tumors treated with SS1-KIRS2/DAP12, SS1-28ζ, and SS1-41BBζ CAR T cells had $hCD45^+$ TILs that comprised 2–4% of the total viable cells within the tumor with comparable frequencies for each group (Fig 4A). Immunohistochemical staining showed abundant $CD8^+$ (Fig 4B) and $CD4^+$ TILs (data not shown) within the tumors of SS1-KIRS2/DAP12, SS1-28ζ, and SS1-41BBζ CAR T cell-treated mice confirming the flow cytometric analysis. The increased efficacy of the SS1-KIRS2/DAP12 T cells is therefore not due to increased TIL frequency within the tumors at late stages of tumor growth. Only mice receiving the SS1-BBζ CAR T cells had detectable human $CD45^+$ ($hCD45^+$) cells in the blood and spleen (Fig 4C) consistent with the previously observed effect of the 4-1BB costimulatory domain on *in vivo* CAR^+ T-cell persistence (5).

Since the comparison of TILs was limited by the large differences in tumor volume at the late time points in our early experiments, we sought to examine TILs isolated at earlier time points following T-cell injection. Evaluation of TILs at 10 days following T-cell injection demonstrated comparable frequencies of $hCD45^+$ TILs within tumors treated with SS1-28ζ and SS1-KIRS2/DAP12 CAR T cells; however, few $CD45^+$ TILs were present in the SS1-BBζ CAR T-cell group (Fig 5A). Limited analysis of the isolated TILs showed that only SS1-KIRS2/DAP12-modified T cells were capable of *in vitro* lytic activity towards EM-meso cells (data not shown). These results suggest that delayed accumulation of SS1-BBζ T cells into the tumor along with tumor-induced hypofunction contribute to the poor antitumor activity of these cells despite their high frequency at later stages of tumor development. A repeat experiment was conducted comparing SS1-28ζ and SS1-KIRS2/DAP12 T cells with TIL isolation at 18 days following T-cell injection to obtain greater numbers of TILs for phenotypic and functional analysis (Fig 5B). Isolated SS1-28ζ TILs demonstrated markedly reduced cytotoxic activity and antigen-specific IFNγ production compared to cryopreserved T cells used for treatment. In contrast, TILs from SS1-KIRS2/DAP12-modified T cell-treated tumors showed comparable *in vitro* cytotoxicity and IFNγ production to cryopreserved cells (Fig 5C and 5D, respectively).

The potential mechanisms by which T cells might lose function within a TME are many; however, loss of CAR expression is one potential explanation that could be readily examined. Immunoblotting of protein lysates from TILs and cryopreserved cells for CAR protein demonstrated loss of SS1-28ζ expression in the recovered TILs (Fig 5E). In contrast,

DAP12 expression in SS1-KIRS2/DAP12 TILs was preserved correlating with the retained function for these isolated TILs (Fig 5F). In a separate experiment, we confirmed the similar loss of SS1-BBζ CAR expression by TILs, and further demonstrate that the loss of SS1-BBζ CAR expression is reversible with *ex vivo* culture of TILs for 24 hours (Fig 5G). These data indicate that CAR loss is an important, and previously unrecognized, mechanism of acquired hypofunction for CD3ζ-based CAR T cells. The retention of CAR and DAP12 expression by TILs explains, at least in part, the enhanced antitumor activity observed with SS1-KIRS2/DAP12-modified T cells.

Discussion

We have shown that a “KIR-CAR” can be simply constructed by swapping the two immunoglobulin-like domains of the KIR2DS2 ectodomain with an scFv capable of binding a desired target antigen. When delivered to T cells together with DAP12, this KIR-based CAR triggers antigen-specific cytotoxicity, cytokine production and proliferation that is comparable to 2nd generation CD3ζ-based CARs *in vitro* without the need for additional domains from costimulatory receptors. The ability of a KIR-based CAR to activate T cells in the absence of added costimulation is interesting in light of the critical importance of costimulation for full T-cell activation and acquisition of effector function. KIR2DS2, the natural KIR upon which the presented KIR-CAR is based, has previously been reported to deliver a costimulation-like signal to T cells. In these studies, engagement of the KIR in T-cell clones lacking DAP12 expression augmented anti-CD3-induced IFNγ production (16). The mechanism of this costimulatory response has not been elucidated, but might be related to interactions between the KIR or DAP12 and other, yet to be identified, adaptor molecules or costimulatory receptors. In particular, integrins are well recognized to provide costimulatory signals to T cells (38, 39). In cellular contexts such as macrophages and neutrophils, DAP12 appears critical to outside-in signaling by integrin receptors (40). The expression of DAP12 in T cells might confer unique signaling activity to LFA-1 and other integrins expressed by T cells, and these effects could underlie some of the enhanced functional activity of T cells expressing SS1-KIRS2/DAP12. Cytokines also deliver important secondary signals to T cells that can augment T-cell activation and differentiation. Bezbradica and colleagues found that Jak2 signaling downstream of the IFNγ receptor is directly coupled to signaling by FcγRI, a related ITAM-based signaling complex, and these interactions regulate the signaling of each pathway (41). Similar integration between DAP12 and the IFNαR signaling has been observed (42). In addition to interactions with the cytokine c-FMS in osteoclast development, DAP12 signaling also interacts with TRAF signaling downstream of the type II TNF receptor, RANKL (43, 44). In aggregate, these studies increasingly demonstrate that ITAM-based adaptor proteins like DAP12 have the potential to interact with diverse, heterologous proteins and modify signaling pathways that are likely to be important in T-cell differentiation and function. It is unknown what role, if any, these processes play in the KIR-CAR system, but exploring these potential interactions will be an important area of future study.

One of the most important findings in this study is that, although T cells engineered to express the mesothelin-specific CD3ζ-based CARs and KIR-CAR/Dap12 showed similar functional activity *in vitro*, KIR-CAR/Dap12-modified T cells were much more effective in

the *in vivo* setting (see Fig 3A). Although interaction with heterologous signaling pathways as discussed above might contribute to the enhanced *in vivo* activity of KIR-CAR/Dap12-modified T cells, we have demonstrated that SS1-KIRS2/DAP12 TILs, unlike CD3ζ-based CARs, retain receptor expression in the TME that correlates with the maintenance of TIL effector function. Enhanced stability of the KIR/DAP12 complex within the plasma membrane following antigen engagement is one potential mechanism to explain the observed difference in CAR expression within TILs. The loss of endogenous CD3ζ expression in TILs has been long recognized, and is associated with loss of T-cell function within the TME (45). TCR/CD3 complex internalization and degradation following antigen engagement are also well-described phenomena in T cells (46, 47). Although the precise mechanism for the loss of CD3ζ expression by TILs has not been fully elucidated, TCR/CD3 receptor complex internalization and degradation following antigen activation combined with metabolic stress within the TME that limits new synthesis of new complex components may contribute to the loss of CD3ζ by TILs (48). The surface expression and recycling of KIRs and DAP12 are less well studied. As we have confirmed with our KIR-based CAR, KIRs do not require assembly into a multi-chain immunoreceptor complex with DAP12 for surface expression, which is distinctly different from TCR that critically depends upon CD3ζ association for surface TCR expression (16, 49, 50). Mulrooney and colleagues made the additional, intriguing observation while studying natural KIRs that internalization and loss of surface KIR expression following receptor crosslinking is reduced in the presence of DAP12 (49). Reduced KIR-CAR internalization and degradation following antigen engagement would therefore provide a potential explanation for the observed difference in receptor expression in freshly isolated TILs. In addition to providing a mechanism for TILs to retain antigen recognition and effector function in the context of continuous ligand exposure, the duration of T-cell engagement with APCs also correlates with T-cell survival and effector function (51). Enhanced surface stability of a KIR-CAR might therefore contribute to the costimulation-independent stimulatory activity observed with the KIR-based CAR system by permitting more sustained interactions with antigen-positive target cells and longer duration of receptor signaling.

Eshhar and colleagues first described the single molecule CAR design in 1993 (52). This design has shown great utility in adoptive T-cell immunotherapy; however, the vast majority of research on CARs to date has focused upon the modification of this single chain receptor design with introduction of domains from other costimulatory receptors like CD28 and 4-1BB to enhance function. The results presented here show that alternative CAR designs, especially multi-chain designs incorporating alternative ITAM-containing adaptor proteins beyond CD3ζ, are worthy of future exploration, especially in solid malignancies in which T cells with CD3ζ-based CARs have shown limited clinical activity to date.

Supplementary Material

Refer to Web version on PubMed Central for supplementary material.

Acknowledgments

The authors would like to thank Carl June at the University of Pennsylvania for his helpful review of the manuscript.

Funding: The work presented was funded through a grant from the NIH Common Fund (1PN1EY016586) with additional support from Novartis.

References

1. Sadelain M, Brentjens R, Riviere I. The basic principles of chimeric antigen receptor design. Cancer Discov. 2013; 3:388–98. [PubMed: 23550147]
2. Finney HM, Akbar AN, Lawson AD. Activation of resting human primary T cells with chimeric receptors: costimulation from CD28, inducible costimulator, CD134, and CD137 in series with signals from the TCR zeta chain. J Immunol. 2004; 172:104–13. [PubMed: 14688315]
3. Maher J, Brentjens RJ, Gunset G, Riviere I, Sadelain M. Human T-lymphocyte cytotoxicity and proliferation directed by a single chimeric TCRzeta/CD28 receptor. Nat Biotechnol. 2002; 20:70–5. [PubMed: 11753365]
4. Carpenito C, Milone MC, Hassan R, Simonet JC, Lakhal M, Suhoski MM, et al. Control of large, established tumor xenografts with genetically retargeted human T cells containing CD28 and CD137 domains. Proce Natl Acad Sci U S A. 2009; 106:3360–5.
5. Milone MC, Fish JD, Carpenito C, Carroll RG, Binder GK, Teachey D, et al. Chimeric receptors containing CD137 signal transduction domains mediate enhanced survival of T cells and increased antileukemic efficacy in vivo. Mol Ther. 2009; 17:1453–64. [PubMed: 19384291]
6. Barrett DM, Singh N, Porter DL, Grupp SA, June CH. Chimeric antigen receptor therapy for cancer. Annu Rev Med. 2014; 65:333–47. [PubMed: 24274181]
7. Sigalov AB. Evolution of immunity: no development without risk. Immunol Res. 2012; 52:176–81. [PubMed: 22095544]
8. Sigalov AB. Multichain immune recognition receptor signaling from spatiotemporal organization to human disease. Preface. Adv Exp Med Biol. 2008; 640:ix–xi. [PubMed: 19065778]
9. Brocker T. Chimeric Fv-zeta or Fv-epsilon receptors are not sufficient to induce activation or cytokine production in peripheral T cells. Blood. 2000; 96:1999–2001. [PubMed: 10961908]
10. Brocker T, Karjalainen K. Signals through T cell receptor-zeta chain alone are insufficient to prime resting T lymphocytes. J Exp Med. 1995; 181:1653–9. [PubMed: 7722445]
11. Thielens A, Vivier E, Romagne F. NK cell MHC class I specific receptors (KIR): from biology to clinical intervention. Curr Opin Immunol. 2012; 24:239–45. [PubMed: 22264929]
12. Moretta A, Biassoni R, Bottino C, Pende D, Vitale M, Poggi A, et al. Major histocompatibility complex class I-specific receptors on human natural killer and T lymphocytes. Immunol Rev. 1997; 155:105–17. [PubMed: 9059886]
13. Falk CS, Nossner E, Frankenberger B, Schendel DJ. Non-MHC-restricted CD4+ T lymphocytes are regulated by HLA-Cw7-mediated inhibition. Hum Immunol. 2000; 61:1219–32. [PubMed: 11163077]
14. Remtoula N, Bensussan A, Marie-Cardine A. Cutting edge: selective expression of inhibitory or activating killer cell Ig-like receptors in circulating CD4+ T lymphocytes. J Immunol. 2008; 180:2767–71. [PubMed: 18292496]
15. Lanier LL, Corliss BC, Wu J, Leong C, Phillips JH. Immunoreceptor DAP12 bearing a tyrosine-based activation motif is involved in activating NK cells. Nature. 1998; 391:703–7. [PubMed: 9490415]
16. Snyder MR, Nakajima T, Leibson PJ, Weyand CM, Goronzy JJ. Stimulatory killer Ig-like receptors modulate T cell activation through DAP12-dependent and DAP12-independent mechanisms. J Immunol. 2004; 173:3725–31. [PubMed: 15356118]
17. Wang LC, Lo A, Scholler J, Sun J, Majumdar RS, Kapoor V, et al. Targeting fibroblast activation protein in tumor stroma with chimeric antigen receptor T cells can inhibit tumor growth and augment host immunity without severe toxicity. Cancer Immunol Res. 2014; 2:154–66. [PubMed: 24778279]
18. Barrett DM, Zhao Y, Liu X, Jiang S, Carpenito C, Kalos M, et al. Treatment of advanced leukemia in mice with mRNA engineered T cells. Hum Gene Ther. 2011; 22:1575–86. [PubMed: 21838572]
19. Moon EK, Wang LC, Dolfi DV, Wilson CB, Ranganathan R, Sun J, et al. Multifactorial T-cell Hypofunction That Is Reversible Can Limit the Efficacy of Chimeric Antigen Receptor-

Transduced Human T cells in Solid Tumors. Clin Cancer Res. 2014; 20:4262–73. [PubMed: 24919573]

20. Call ME, Wucherpfennig KW, Chou JJ. The structural basis for intramembrane assembly of an activating immunoreceptor complex. Nat Immunol. 2010; 11:1023–9. [PubMed: 20890284]
21. Varela-Rohena A, Molloy PE, Dunn SM, Li Y, Suhoski MM, Carroll RG, et al. Control of HIV-1 immune escape by CD8 T cells expressing enhanced T-cell receptor. Nat Med. 2008; 14:1390–5. [PubMed: 18997777]
22. Okamoto S, Mineno J, Ikeda H, Fujiwara H, Yasukawa M, Shiku H, et al. Improved expression and reactivity of transduced tumor-specific TCRs in human lymphocytes by specific silencing of endogenous TCR. Cancer Res. 2009; 69:9003–11. [PubMed: 19903853]
23. Kowolik CM, Topp MS, Gonzalez S, Pfeiffer T, Olivares S, Gonzalez N, et al. CD28 costimulation provided through a CD19-specific chimeric antigen receptor enhances in vivo persistence and antitumor efficacy of adoptively transferred T cells. Cancer Res. 2006; 66:10995–1004. [PubMed: 17108138]
24. Pule MA, Straathof KC, Dotti G, Heslop HE, Rooney CM, Brenner MK. A chimeric T cell antigen receptor that augments cytokine release and supports clonal expansion of primary human T cells. Mol Ther. 2005; 12:933–41. [PubMed: 15979412]
25. Brentjens RJ, Latouche JB, Santos E, Marti F, Gong MC, Lyddane C, et al. Eradication of systemic B-cell tumors by genetically targeted human T lymphocytes co-stimulated by CD80 and interleukin-15. Nat Med. 2003; 9:279–86. [PubMed: 12579196]
26. Friedmann-Morvinski D, Bendavid A, Waks T, Schindler D, Eshhar Z. Redirected primary T cells harboring a chimeric receptor require costimulation for their antigen-specific activation. Blood. 2005; 105:3087–93. [PubMed: 15626734]
27. Maude SL, Frey N, Shaw PA, Aplenc R, Barrett DM, Bunin NJ, et al. Chimeric antigen receptor T cells for sustained remissions in leukemia. N Engl J Med. 2014; 371:1507–17. [PubMed: 25317870]
28. Porter DL, Levine BL, Kalos M, Bagg A, June CH. Chimeric antigen receptor-modified T cells in chronic lymphoid leukemia. N Engl J Med. 2011; 365:725–33. [PubMed: 21830940]
29. Yuan D, Liu B, Liu K, Zhu G, Dai Z, Xie Y. Overexpression of fibroblast activation protein and its clinical implications in patients with osteosarcoma. J Surg Oncol. 2013; 108:157–62. [PubMed: 23813624]
30. Arnold JN, Magiera L, Kraman M, Fearon DT. Tumoral immune suppression by macrophages expressing fibroblast activation protein-alpha and heme oxygenase-1. Cancer Immunol Res. 2014 Feb.2:121–6. [PubMed: 24778275]
31. Jacob M, Chang L, Pure E. Fibroblast activation protein in remodeling tissues. Curr Mol Med. 2012; 12:1220–43. [PubMed: 22834826]
32. Kraman M, Bambrough PJ, Arnold JN, Roberts EW, Magiera L, Jones JO, et al. Suppression of antitumor immunity by stromal cells expressing fibroblast activation protein-alpha. Science. 2010; 330:827–30. [PubMed: 21051638]
33. Loeffler M, Kruger JA, Niethammer AG, Reisfeld RA. Targeting tumor-associated fibroblasts improves cancer chemotherapy by increasing intratumoral drug uptake. J Clin Invest. 2006; 116:1955–62. [PubMed: 16794736]
34. Lee J, Fassnacht M, Nair S, Boczkowski D, Gilboa E. Tumor immunotherapy targeting fibroblast activation protein, a product expressed in tumor-associated fibroblasts. Cancer Res. 2005; 65:11156–63. [PubMed: 16322266]
35. Ostermann E, Garin-Chesa P, Heider KH, Kalat M, Lamche H, Puri C, et al. Effective immunoconjugate therapy in cancer models targeting a serine protease of tumor fibroblasts. Clin Cancer Res. 2008; 14:4584–92. [PubMed: 18628473]
36. Tran E, Chinnasamy D, Yu Z, Morgan RA, Lee CC, Restifo NP, et al. Immune targeting of fibroblast activation protein triggers recognition of multipotent bone marrow stromal cells and cachexia. J Exp Med. 2013; 210:1125–35. [PubMed: 23712432]
37. Roberts EW, Deonarine A, Jones JO, Denton AE, Feig C, Lyons SK, et al. Depletion of stromal cells expressing fibroblast activation protein-alpha from skeletal muscle and bone marrow results in cachexia and anemia. J Exp Med. 2013; 210:1137–51. [PubMed: 23712428]

38. Zuckerman LA, Pullen L, Miller J. Functional consequences of costimulation by ICAM-1 on IL-2 gene expression and T cell activation. J Immunol. 1998; 160:3259–68. [PubMed: 9531282]
39. Van Seventer GA, Shimizu Y, Horgan KJ, Shaw S. The LFA-1 ligand ICAM-1 provides an important costimulatory signal for T cell receptor-mediated activation of resting T cells. J Immunol. 1990; 144:4579–86. [PubMed: 1972160]
40. Mocsai A, Abram CL, Jakus Z, Hu Y, Lanier LL, Lowell CA. Integrin signaling in neutrophils and macrophages uses adaptors containing immunoreceptor tyrosine-based activation motifs. Nat Immunol. 2006; 7:1326–33. [PubMed: 17086186]
41. Bezbradica JS, Rosenstein RK, DeMarco RA, Brodsky I, Medzhitov R. A role for the ITAM signaling module in specifying cytokine-receptor functions. Nat Immunol. 2014; 15:333–42. [PubMed: 24608040]
42. Wang L, Tassiulas I, Park-Min KH, Reid AC, Gil-Henn H, Schlessinger J, et al. 'Tuning' of type I interferon-induced Jak-STAT1 signaling by calcium-dependent kinases in macrophages. Nat Immunol. 2008; 9:186–93. [PubMed: 18084294]
43. Koga T, Inui M, Inoue K, Kim S, Suematsu A, Kobayashi E, et al. Costimulatory signals mediated by the ITAM motif cooperate with RANKL for bone homeostasis. Nature. 2004; 428:758–63. [PubMed: 15085135]
44. Zou W, Reeve JL, Liu Y, Teitelbaum SL, Ross FP. DAP12 couples c-Fms activation to the osteoclast cytoskeleton by recruitment of Syk. Mol Cell. 2008; 31:422–31. [PubMed: 18691974]
45. Mizoguchi H, O'Shea JJ, Longo DL, Loeffler CM, McVicar DW, Ochoa AC. Alterations in signal transduction molecules in T lymphocytes from tumor-bearing mice. Science. 1992; 258:1795–8. [PubMed: 1465616]
46. Valitutti S, Muller S, Salio M, Lanzavecchia A. Degradation of T cell receptor (TCR)-CD3-zeta complexes after antigenic stimulation. J Exp Med. 1997; 185:1859–64. [PubMed: 9151711]
47. Liu H, Rhodes M, Wiest DL, Vignali DA. On the dynamics of TCR:CD3 complex cell surface expression and downmodulation. Immunity. 2000; 13:665–75. [PubMed: 11114379]
48. Rodriguez PC, Ochoa AC. Arginine regulation by myeloid derived suppressor cells and tolerance in cancer: mechanisms and therapeutic perspectives. Immunol Rev. 2008; 222:180–91. [PubMed: 18364002]
49. Mulrooney TJ, Posch PE, Hurley CK. DAP12 impacts trafficking and surface stability of killer immunoglobulin-like receptors on natural killer cells. J Leukoc Biol. 2013; 94:301–13. [PubMed: 23715743]
50. Roberts JL, Lauritsen JP, Cooney M, Parrott RE, Sajaroff EO, Win CM, et al. T-B+NK+ severe combined immunodeficiency caused by complete deficiency of the CD3zeta subunit of the T-cell antigen receptor complex. Blood. 2007; 109:3198–206. [PubMed: 17170122]
51. Gett AV, Sallusto F, Lanzavecchia A, Geginat J. T cell fitness determined by signal strength. Nat Immunol. 2003; 4:355–60. [PubMed: 12640450]
52. Eshhar Z, Waks T, Gross G, Schindler DG. Specific activation and targeting of cytotoxic lymphocytes through chimeric single chains consisting of antibody-binding domains and the gamma or zeta subunits of the immunoglobulin and T-cell receptors. Proc Natl Acad Sci U S A. 1993; 90:720–4. [PubMed: 8421711]

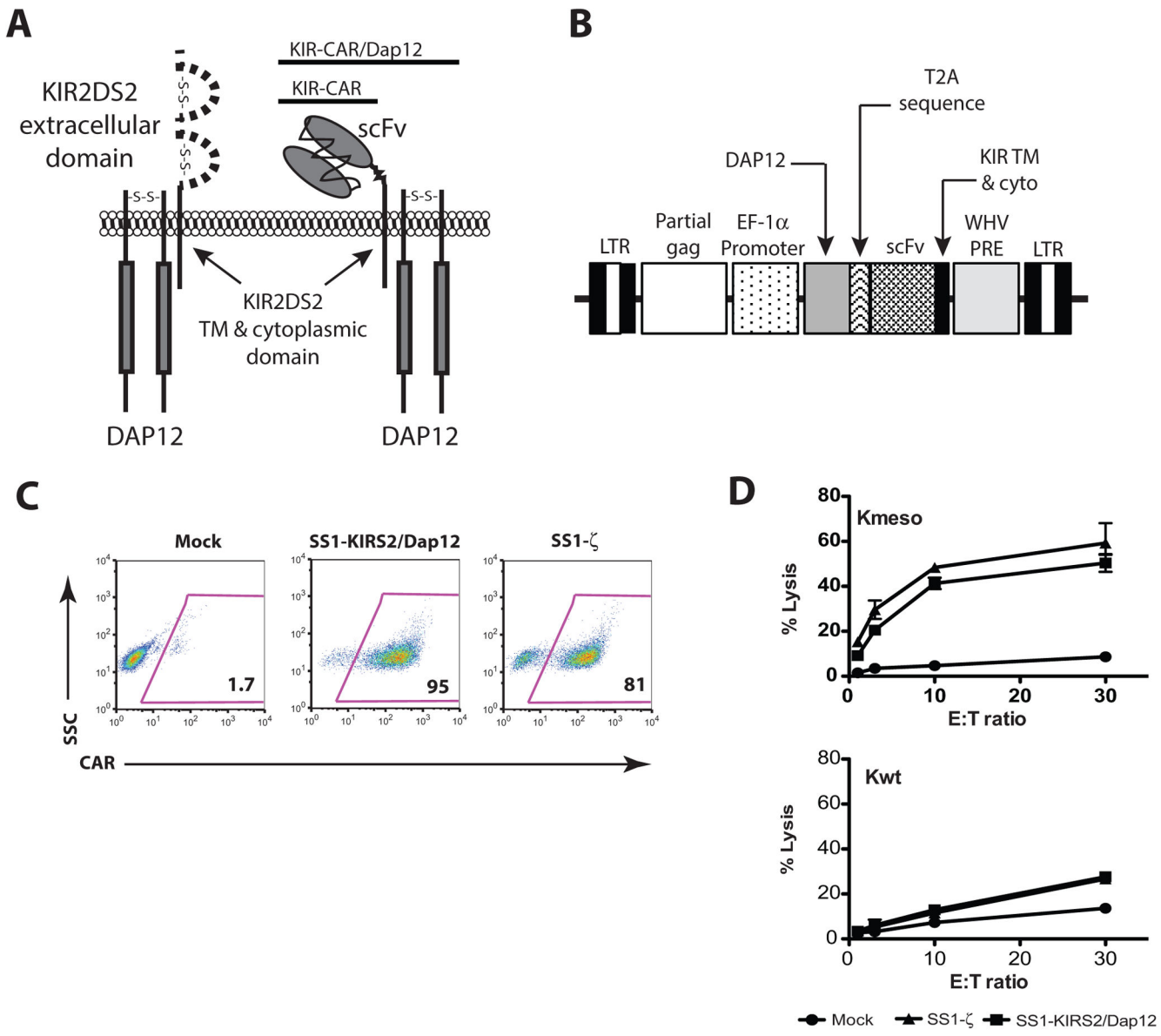

Figure 1. KIR-CARs/Dap12 trigger robust antigen-specific cytotoxicity *in vitro*

A) Schematic diagram of a mesothelin-specific KIR–CAR. B) Schematic diagram of the lentiviral vector used for co-delivery of a KIR-CAR and DAP12. C) Primary human T cells were simulated with anti-CD3/anti-CD28 T-cell activator beads (Dynabeads® CD3/CD28 CTS™, Life Technologies). After 24 hrs of stimulation, the T cells were transduced with a lentiviral vector encoding the indicated CAR or mock-transduced (Mock). Cells were expanded for 9 days, and analyzed by flow cytometry for the expression of the indicated CAR using biotinylated goat-anti-mouse $F(ab)_2$ followed by streptavidin-PE. Results are representative of at least 3 independent experiments. D) Antigen-specific cytotoxic activity of T cells generated as described in panel C was assessed by a 4-hr ^{51}Cr-release assay as described in the supplemental materials and methods using K562 cells (Kwt) or K562 cells engineered to express human mesothelin (Kmeso).

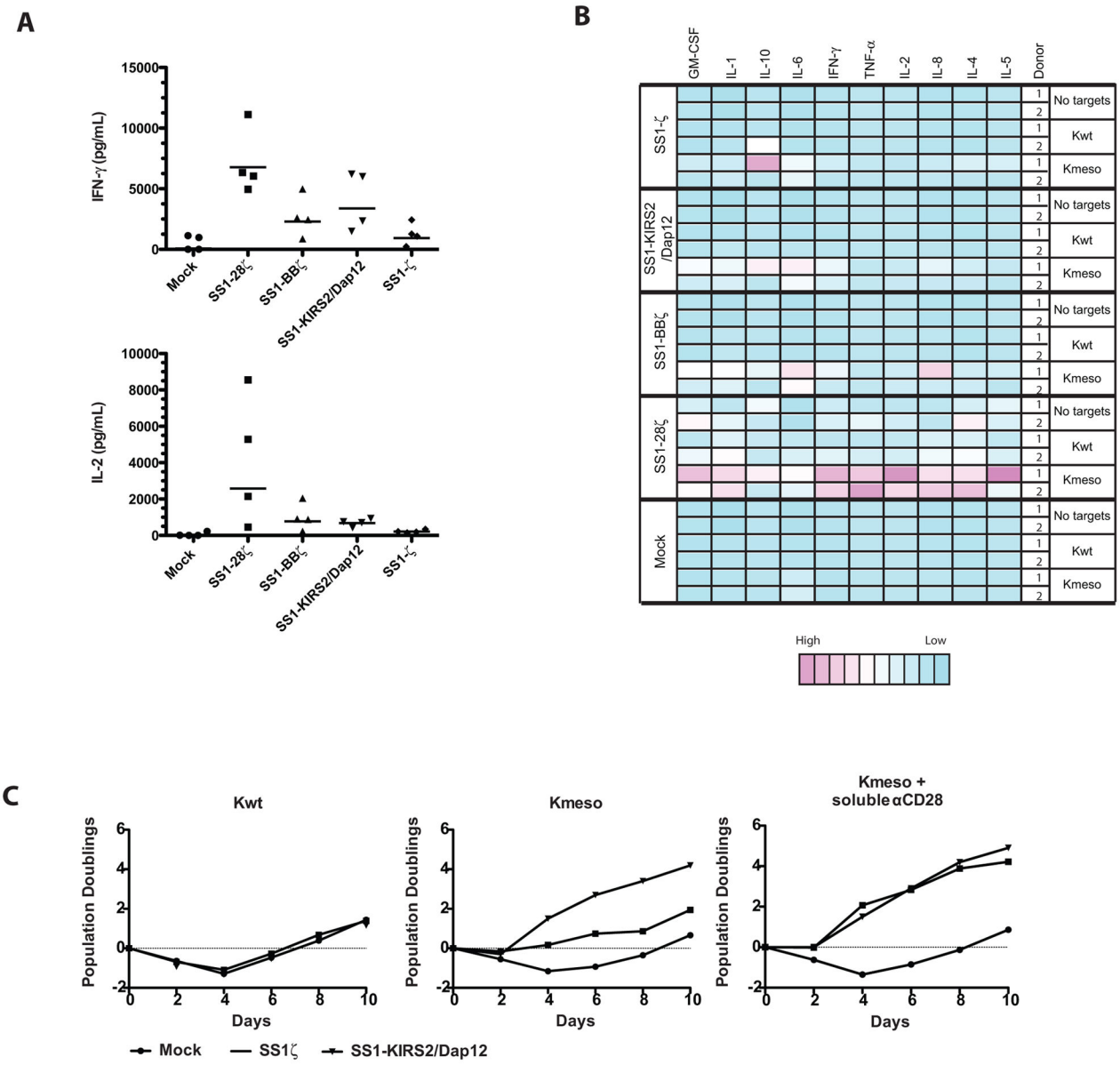

Figure 2. A KIR-CAR/Dap12 induces cytokine secretion and T-cell proliferation that is comparable to CD3ζ-based CARs with costimulatory signals

Primary human T cells were simulated, transduced as indicated and expanded as described in Figure 1. Following expansion, the transduced T cells were mixed with Kwt or Kmeso at a ratio of 2:1 A) Cytokine concentrations in supernatants following 24 hours of stimulation were determined by ELISA for the indicated cytokines in multiple independent donors. Repeated measure ANOVA demonstrated a statistically significant CAR effect on IFNγ ($p=0.002$) and IL2 ($p=0.016$). SS1-KIRS2/DAP12 vs. mock for IFNγ (post-hoc paired t-test, $p = 0.016$). SS1-KIRS2/Dap12 vs. SS1-28ζ for IL2 (post-hoc paired t-test, $p=0.041$) B) Cytokine concentrations in supernatants were assessed by a multiplex luminex-based immunoassay (Cytokine Human 10-Plex Panel, Life Technologies used according to manufacturer's instructions). A heatmap of relative concentration after normalization across

donor and conditions to the lowest concentration for each cytokine was generated using the heatmap package implement in R statistical software. C) Following the initial expansion, T cells were restimulated with γ-irradiated Kwt stimulator cells (negative control) or Kmeso with or without soluble anti-CD28 agonist antibody (1-μg/mL) as indicated. Viable T cells were enumerated by flow cytometry-based counting using CountBright counting beads (BD Biosciences) and 7-AAD, and population doublings was calculated relative to the starting T-cell number.

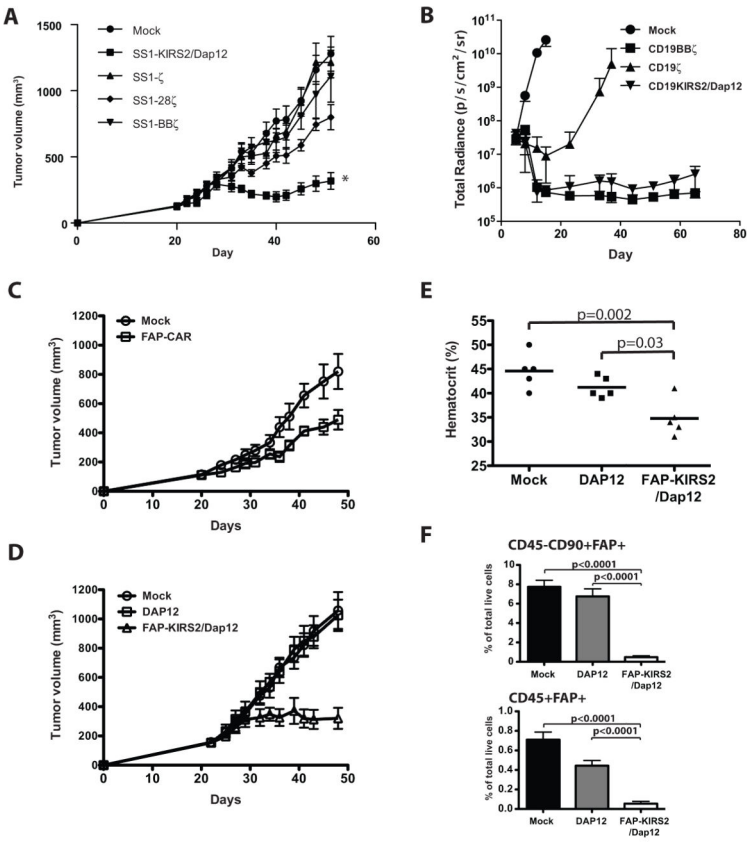

Figure 3. T cells expressing a KIR-CAR/Dap12 show potent *in vivo* antitumor activity that is resistance to the tumor-induced T-cell hypofunction observed with CD3ζ-based CARs

A) Adult NSG mice were injected subcutaneously with 2×10^6 EM-meso cells as described previously (19). 5×10^6 primary human T cells transduced with the indicated CARs (80–90% transduction efficiency) were injected intravenously (IV) on day 20 following tumor implantation. Tumor volume was measured by caliper using the formula $(\pi/6) \times (\text{length}) \times (\text{width})^2$ at the indicated times (n = 7 mice per group). Tumor volume was compared across CAR T-cell treatment groups at day 40 (nadir of tumor regression) and day 52 (end of the experiment) by a one-way ANOVA ($p < 0.001$) with between-group comparisons performed by a post-hoc Scheffe F-test. * indicates statistically different from the mock control at both time points ($p < 0.001$). (B) NSG mice were engrafted with CBG-labeled Nalm6 leukemic cells as described in the materials and methods. 2×10^6 primary human T cells transduced with the indicated CAR (70–90% transduction efficiency) were injected IV on day 5 following leukemic cell line injection. Tumor burden was assessed via bioluminescent imaging at the indicated times (n = 5 mice per group). Greater than 50% of the mice treated with mock-transduced and CD19ζ-transduced T cells developed terminal leukemia requiring sacrifice on days 15 and 37, respectively. Greater than 50% of the mice treated with CD19BBζ-transduced T cells developed graft-vs-host disease requiring termination of the experiment on day 72. Total radiance was compared across the CAR T-cell treatment groups at day 37 by a one-way ANOVA ($p < 0.001$) with between-group comparisons performed by a post-hoc Scheffe F-test. CD19BBζ– and CD19KIRS2/DAP12-transduced T-cell groups were statistically different from the CD19ζ-transduced T-cell group ($p < 0.001$), but no

difference could be demonstrated between the CD19BBζ and CD19KIRS2/Dap12 groups (p=0.748). (C) NSG mice were injected subcutaneously with EM-meso cells as described in panel A. T cells transduced with FAP-BBζ (FAP-CAR) or mock transduced were injected intravenously on day 20. Tumor volume was measured as in panel A. FAP-BBζ T cell-treated mice showed statistically significantly delayed tumor growth compared with mock-treated control tumors ($p<0.026$, Student's t test). N=5 animals per group. (D) NSG mice were injected subcutaneously with EM-meso cells as described in panel A. T cells transduced with DAP12 alone, FAP-KIR/DAP12 or mock transduced were injected intravenously on day 21. Tumor volume was measured as in panel A. Tumors from FAP-KIR/DAP12 T cell-treated mice shows significantly delayed growth with tumor volume significantly reduced compared to DAP12 and mock controls on day 48 ($p<0.01$, ANOVA with post-hoc Scheffe F-test). N=5 animals per group. (E) Hematocrit was measured on blood collected from mice shown in Fig 3D on day 48. Treatment conditions were compared using an ANOVA with post-hoc Scheffe F-test with the p-values shown. (F) Flow cytometry was performed on tumors harvested on day 48 from 5 animals shown in panel C. The frequency of $CD45^{-}CD90^{+}FAP^{+}$ and $CD45^{+}FAP^{+}$ cells within the tumor were compared by ANOVA with the p-values indicated.

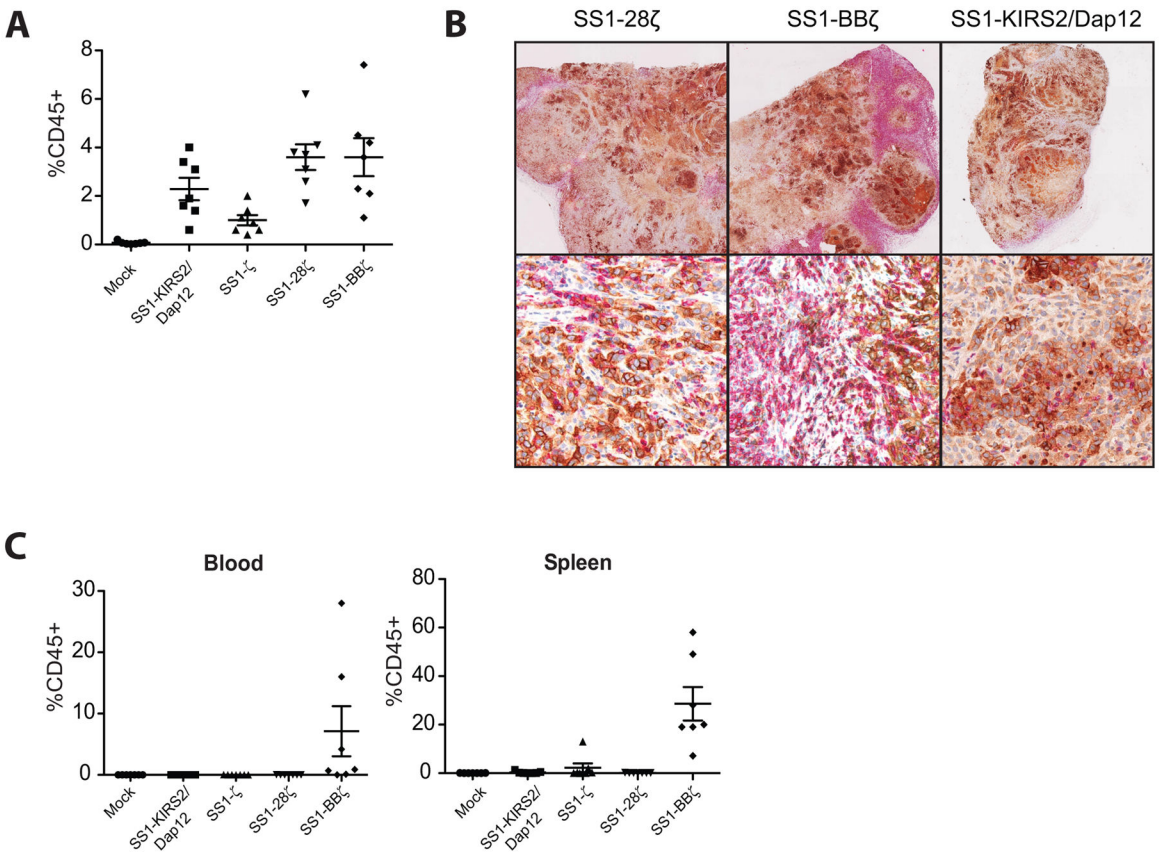

Figure 4. TIL frequency does not correlated with the enhanced KIR-CAR/Dap12 activity *in vivo*

A) The frequency of viable human lymphocytes was assessed by flow cytometry using staining for human CD45 (hCD45) and a viability marker (7-AAD) in tumor following *in vitro* enzymatic digestion (described in detail in the material and methods). $hCD45^+$ cell frequencies were compared by a one-way ANOVA with between-group comparisons performed by a post-doc Tukey's multiple comparison test as implemented in Prism (GraphPad, v 5.1). $hCD45^+$ cell frequencies in tumors of SS128ζ, SS1BBζ- and SS1-KIRS2/DAP12-treated mice were significantly higher than mock-treated mice with SS1-28ζ and SS1-BBζ-treated mice also exhibiting higher frequencies compared to SS1ζ-treated tumors ($p < 0.05$). (B) Portions of tumors from mice shown in Figure 3A collected at the time of sacrifice were fixed in buffered formalin. Immunohistochemistry was performed as described in the material and methods with mesothelin stained in brown and CD8 cells stained in red. Slides were counterstained with hematoxylin. Low power (top row) and high power (bottom row) fields from 3 representative tumors analyzed from each treatment group are shown as indicated.

(C) The frequency of viable human lymphocytes was assessed by flow cytometry as described in panel B in whole blood and spleen from the mice described in panel A. $hCD45^+$ cells were significantly more frequent in the blood and spleens of SS1BBζ-treated mice compared to those treated with mock-transduced T cells ($p < 0.05$).

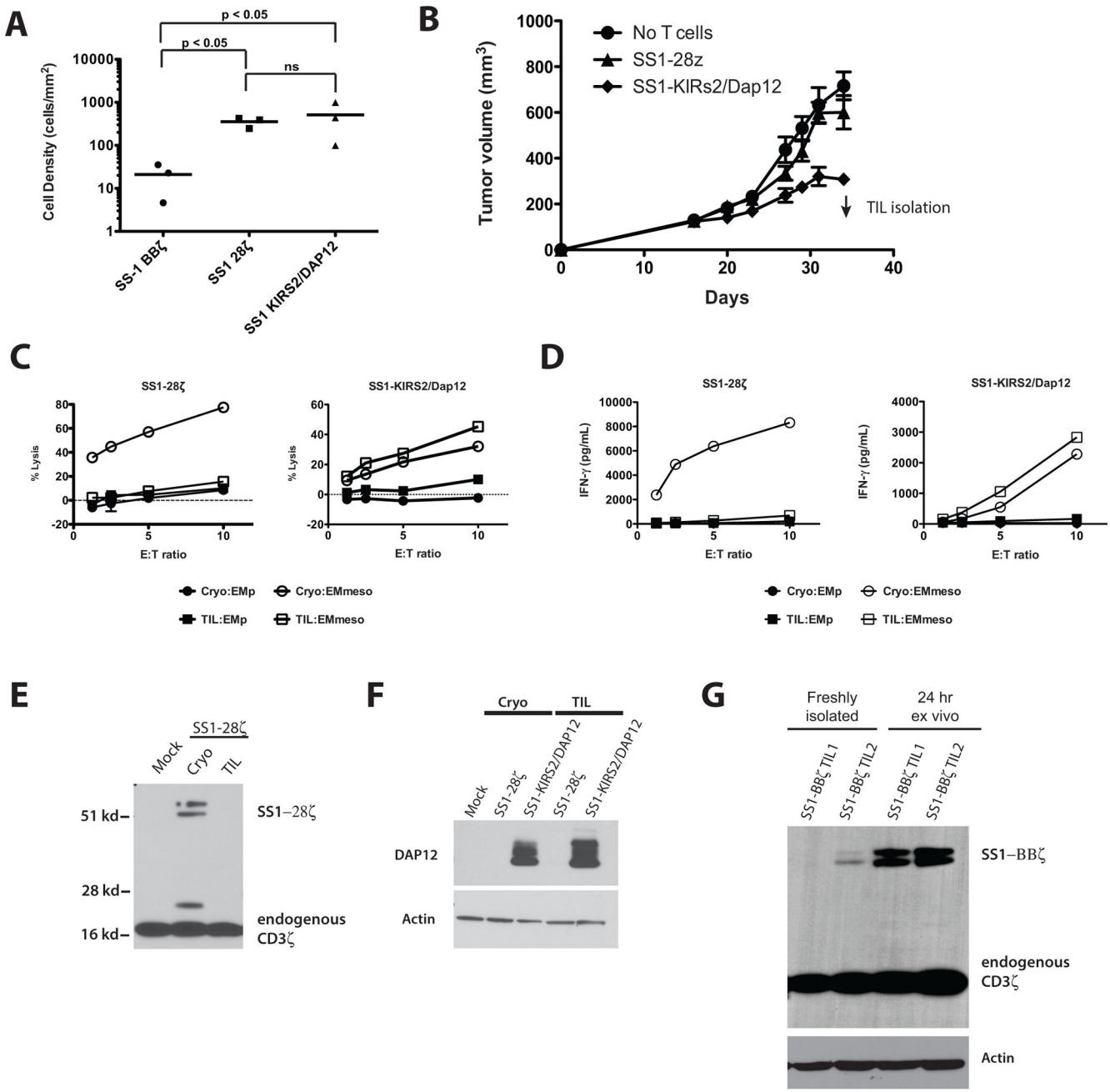

Figure 5. Retention of KIR-CAR/Dap12 expression in TILs is associated with resistance to tumor-induced hypofunction

A) Adult NSG mice were injected subcutaneously with 2×10^6 EM-meso cells followed by 5×10^6 CAR T cells on day 20. The density of $CD8^+$ human lymphocytes within tumors at 10 days following CAR T infusion (day 30 of tumor growth) was determined by immunohistochemistry for human CD8 alpha (clone C8/144B; #M7103; Dako) and mesothelin (clone 5B2; #MS-1320; Thermo Scientific) and automated image analysis as described in the supplemental methods. Cell density was compared among the CAR-modified T-cell groups following $\log_{10}$ transformation of the cell density data using a one-

way ANOVA followed by a post-hoc Tukey test as implemented in Prism (GraphPad, version 5.0). B), Adult NSG mice were injected subcutaneously with EM-meso cells followed by the indicated CAR T cells (80–90% transduction efficiency, 5×10^6 cells/mouse) on day 20. The arrow indicates the time of TIL isolation used for functional and phenotypic analysis. C) Antigen-specific cytotoxic activity of TILs isolated from the mice described in panel B was assessed by co-culture with firefly luciferase expressing EM-meso cells or EMp cells (parental EM cells lacking mesothelin expression) at the indicated E:T ratios for 18 hours as previously described (19). (D) TILs as described in panel C were mixed with EM-meso or EMp cells at the indicated effector to target (E:T) ratio. A human IFNγ-specific ELISA (R&D systems) was used to determine the IFNγ concentration in supernatants collected at 20 hours following mixing with target cells. E) Western blotting of protein lysates from the TILs described in panels C and D for CD3ζ (clone 6B10.2; sc-1239; Santa Cruz Biotechnology) was performed as described in the supplemental materials and methods. F) Western blotting of protein lysates from the TILs described in panels C and D for DAP12 (clone D7G1X; #12492; Cell Signaling Technology) and β-actin (polyclonal; #AV52099; Sigma-Aldrich). (G) Western blotting for CD3ζ in protein lysates from TILs collected from NSG mice bearing EM-meso tumors on day 31 following treatment with SS1-BBζ CAR T cells. TILs lysates were generated immediately following isolation (freshly isolated) or following 24 hours of *ex vivo* culture in serum-containing RPMI medium (24 hr *ex vivo*).